FISEVIER

Contents lists available at ScienceDirect

Resources, Conservation & Recycling

journal homepage: www.elsevier.com/locate/resconrec





Reducing the environmental impacts of aluminum extrusion

Gregory Oberhausen^a, Yongxian Zhu^a, Daniel R. Cooper^{a,*}

^a Mechanical Engineering Department, University of Michigan, George G. Brown Laboratory, 2350 Hayward Street, Ann Arbor, MI, 48109-2125, USA

ARTICLE INFO

Keywords:
Material flow analysis
Cost modeling
Material efficiency
Sustainable manufacturing
Industrial sustainability
Greenhouse gas emissions
Process scrap

ABSTRACT

The aluminum extrusion industry is growing rapidly; however, there has been little work on quantifying or reducing extrusion's environmental impacts. This article first derives cradle-to-gate cumulative energy demand, greenhouse gas emission, and cost models for direct aluminum extrusion using data collected from extrusion companies, life cycle inventory measurements (e.g., electricity demand) from our own case studies, and physicsbased extrapolations. These models show there is significant scope for increasing both the process energy and material efficiency; however, only increasing the material efficiency will lead to significant environmental benefits and cost savings. Subsequently, an alloy-shape-application material flow analysis of the 2018 North American extrusion industry is conducted to highlight opportunities for improved material utilization throughout the supply chain. Material flow data were collated from existing academic and gray literature in addition to semi-structured interviews with North American extrusion experts. The material flow analysis reveals that around 40% of all aluminum cast into extrusion billets is scrapped before completion in a fabricated product, which increases the cost of the fabricated profile by approximately 16% and the greenhouse gas emissions and cumulative energy demand by approximately 40%. Most of this scrap is created by removing structural and surface finish extrusion defects that are inherent to the current process. Process adaptations that might reduce the material scrapped due to these defects are identified and discussed. Even a 10% reduction in extrusion process forming scrap could save the North American (U.S. and Canada) extrusion industry 270-311 million USD per year and prevent the release of 0.5–2.3 Mt.CO $_{\mathrm{2eq}}$ annually.

1. Introduction

Production of just five key materials (aluminum, steel, cement, paper, and plastic) accounts for over half of all the greenhouse gas (GHG) emissions released by industry worldwide each year (Sutherland et al., 2020). Primary aluminum making is by far the most emissions intensive of these materials per unit of production (Argonne National Laboratory, 2020). Further GHG emissions are released downstream of aluminum production in manufacturing processes that shape, heat treat, join, and finish aluminum components (Seow et al., 2013). Additional environmental concerns include the loss of land to bauxite mining operations and accidental toxic releases such as of red mud produced in the Bayer process for refining aluminum ore (Metson, 2011; BBC, 2010).

Emissions released from aluminum supply chains must be reduced to help prevent the worst consequences of climate change (Allwood et al., 2012; Cann et al., 2020). There are, however, limited opportunities to improve the aluminum production process where the energy efficiency is approaching the thermodynamic limit (Allwood et al., 2010;

Gutowski et al., 2013) and where the GHG emissions intensity has increased in recent years due to the rapid global shift to Chinese production, where 90% of the aluminum-making electricity is generated using emissions-intensive coal (International Aluminum Institute, 2021; Cooper et al., 2017). Reducing aluminum material and energy requirements in downstream manufacturing is therefore a priority.

This article focuses on the aluminum extrusion supply chain because of its significance to the overall industry. Cullen and Allwood's (2013) material flow analysis (MFA) shows that around a fifth of all the aluminum produced worldwide in 2007 was extruded. More recently, Bertram et al's (2017) dynamic MFA shows that global demand for extrusion ingot has grown rapidly since 2000 and, by 2014, far exceeded demand for casting ingots and was comparable to rolled ingot demand. In 2017, 28 Mt of extruded aluminum profiles were produced globally (Rodriguez León and Stark, 2018). These profiles were used across construction (e.g., commercial façade and window frames), transport (e.g., bumper components), equipment (e.g., ladders and scaffolding), consumer durables (e.g., air conditioner tubing), and electronics (e.g.,

E-mail address: drcooper@umich.edu (D.R. Cooper).

^{*} Corresponding author.

extruded plates milled to make laptop enclosures) (Misiolek and Kelly, 2005; Sherman, 2009). Aluminum extrusion is increasingly popular because it permits the use of part-consolidated lightweight profiles with optimized cross-sections, integrated connections, and a high quality surface finish that can be further enhanced with anodizing or powder coating (Misiolek and Kelly, 2005). Aluminum's high thermal conductivity combined with the ability to extrude high surface area profiles makes it an attractive choice for heat sinks and as structural material enclosing electronics.

In a typical direct extrusion plant, long (\approx 7 m), homogenized, direct chill (DC) cast aluminum alloy logs (\emptyset 6–12″; \emptyset 152–305 mm) are cut to shorter billet lengths (0.66–1.83 m) (AEC, 2021) which are then preheated (400–550 °C) before being placed in a heated extrusion chamber and pushed through a die using a dummy block and stem attached to a hydraulic ram (Fig. 1). Profiles made from heat treatable alloys may be cooled using a water spray quench curtain as they leave the die. The extruded profiles may subsequently be artificially aged (heat treated) and/or anodized and painted.

1.1. Previous work on the environmental impacts and costs of extrusion

Several efforts have been made in recent years to improve the efficiency and reduce the costs of aluminum extrusion. Recent developments include more efficient burners in billet preheating furnaces (U.S. DOE, 2003; Wünning, 2007) and start-stop hydraulic pump systems for reducing press electricity requirements (SMS Group, 2020). However, the overall relevance of these developments is not clear without a holistic analysis of the environmental impacts and costs in aluminum extrusion, which can also be used to prioritize future research and development.

Despite the significance of the extrusion industry, there has been little work on quantifying extruded profile environmental impacts or mapping material flows. For example, Haraldsson and Johansson (2018), in a review of measures for improved energy efficiency in aluminum processing, found no academic articles on improving extrusion's energy efficiency across the ten years' worth of publications they examined (2007-2016). Elsewhere, Ingarao et al. (2014) compare the primary energy required to extrude versus machine a given part, and Furu et al. (2017) perform an optimization to find the minimum cost and environmental impacts of aluminum alloys used in the extrusion process by changing only material properties (e.g., yield stress). The most extensive analyses are in the non-peer reviewed literature. The European Aluminum Association (EAA) (European Aluminum Association, 2018) published an environmental profile report based on a survey of 29% of European extruders, and the Aluminum Extruders Council (AEC) (Mulholland, 2016) performed an Environmental Product Declaration (EPD) (ISO, 2016a, 2016b) based on data provided by approximately 33% of North American extruders. The EAA's report presents a limited gate-to-gate Life Cycle Assessment (LCA) from cast billet to extruded profile, excluding the impacts associated with the tooling, lubricant, and capital equipment as well as energy-intensive aluminum production,

casting, and potential post-extrusion processes (e.g., heat-treatment). The AEC's EPD is a cradle-to-gate LCA; it includes the environmental impacts of some tooling (extrusion dies) and finishing processes (e.g., anodizing), and reports the average billet recycled content of survey respondents (54%). The EPD excludes the environmental impact of the lubricant, the capital equipment, or post-extrusion heat-treatment. Both the EAA and AEC studies aggregate energy and material flows (e.g., different scrap flows) and report point values rather than providing predictive models.

Alongside LCA, supply chain MFA is a foundational tool in industrial ecology used to identify scalable opportunities for material efficiency (e. g., increased recycled contents and reduced process yield losses). Other than high-level aluminum industry MFAs (Bertram et al., 2017; Cullen and Allwood, 2013) and a study on the use of aluminum extrusions in French commercial buildings (Billy, 2012), there are to the authors' knowledge no detailed MFAs of the extrusion industry. This forms a significant literature gap given that the AEC EPD found material inputs to be the most significant driver of environmental impacts.

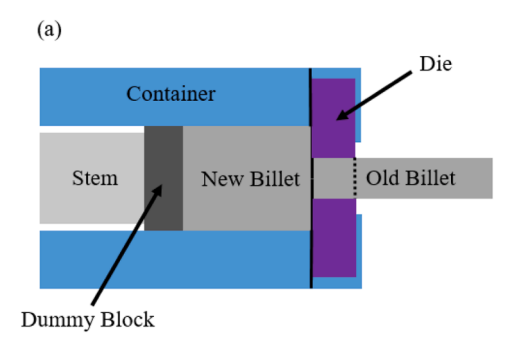
Manufacturing economic analyses are necessary to understand the viability of any proposed process changes that decrease environmental impacts. There have been few attempts at modeling extrusion costs. Low (2009) conducted a case study on the equipment, overhead, material, labor, tooling and maintenance costs for extruding a heatsink profile, finding that production costs were dominated by material costs (66.6%) with equipment depreciation (13.7%), tooling costs (9.9%) and energy costs (5.6%) also significant. Elsewhere, Nieto (2010) developed a feature based cost model for aluminum extrusion to help extrusion die designers predict extrusion profile production costs; however, not all scrap sources are included and energy costs are subsumed in overhead, preventing an energy efficiency cost analysis.

1.2. Scope of work

This work focuses on answering two questions:

- What are the greatest opportunities to reduce the extrusion process' environmental impacts for minimum cost?
- Where are the supply chain opportunities to increase material efficiency?

The first question is answered in Section 2 by creating parametric cradle-to-gate environmental impact and extrusion cost models informed by both industry data and case studies conducted for the purpose of this work. The presented models can be used to make predictions based on as little information as the billet properties and profile geometry. The second question is answered in Section 3 by conducting an alloy-shape-application MFA of the North American extrusion industry. Section 4 then includes a discussion of the opportunities identified in this work and the scale of these opportunities in relation to current industry trends.



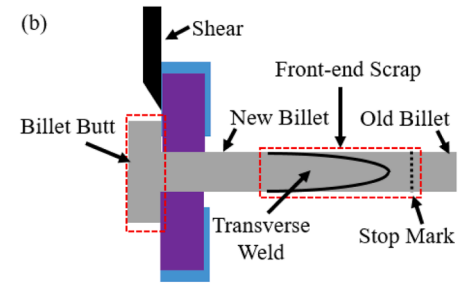


Fig. 1. Schematic of consecutive direct extrusion (a) before and (b) after extrusion of a new billet.

2. Environmental impact and cost models for aluminum extrusion

This section focuses on measuring the electrical power draw of the extrusion process and then evaluating the overall environmental impacts and costs by considering the other inputs and outputs. Subsequently, parametric models are constructed (with uncertainty) that allow the impacts and costs of making any (applicable) part to be predicted.

The environmental impacts are modeled in Umberto (ifu hamburg, 2020) with case study data supplemented by lifecycle inventories based on ecoinvent 3.1 database values (Wernet et al., 2016). The impacts considered are cumulative energy demand (CED), also known as primary or embodied energy, and the cumulative carbon dioxide equivalents emitted, which is a measure of global warming potential (GWP) with a 100-year time horizon. These two environmental indicators have been chosen due to the urgency required to address climate change and because CED is a good proxy for a range of other environmental impacts (Ashby, 2020; Penny et al., 2013). Fig. 2 shows the boundaries of the 'cradle-to-gate' LCAs and cost models. The functional unit is 1 kg of finished extruded profile ready for original equipment manufacturer (OEM) fabrication and assembly. The impacts and costs of tooling and equipment are amortized over the total mass of profiles produced before replacement. In order to reduce confusion, 'MJ' refers to the CED, while 'kWh' and 'therms' refer to delivered (metered) electricity and the energy released from burning natural gas respectively. The indirect costs and impacts from facilities, facility-wide energy requirements (e.g., lighting), administration, and design etc. are not included.

2.1. Case study methodology

Case studies were conducted on a 12 MN Danieli Breda hot direct extrusion press situated at the *Lightweight Innovations for Tomorrow* (LIFT) Manufacturing USA Institute in Detroit, Michigan. Table 1 presents descriptions of the case study profiles and extrusion parameters, and Table S1 describes the equipment.

Electrical power measurements were taken using Fluke 434 (series II) 3-phase power analyzers with a sampling period of 0.25 s. Two material flows were tracked during the case studies: the aluminum billets and the boron nitride lubricant applied to the dummy block face to prevent sticking. In the case studies, aluminum billets (rather than logs) were provided by the metal supplier. A billet cutting process yield loss of 4% was used to account for the process scrap created as a result of the log length typically not being an exact multiple of the billet length (Sheppard, 1999). The other case study scrap sources were the billet butt and front-end defect (transverse weld and stop mark, Fig. 1). The billet butt corresponds to the last 5–15% of an extruded billet, which is typically not extruded through the extrusion die and is instead removed from the container between press strokes by a descending hydraulic

shear and scrapped (Fig. 1). Billet impurities (e.g., oxides, spinels, and intermetallics) are initially dispersed in the billet surface skin but are concentrated in the billet butt during the ram stroke due to the metal flow towards the rear of the billet (Oberhausen et al., 2021). Inclusion of these impurities in the final profile would reduce its esthetic, mechanical and electrical properties (Saha, 2000). Around 7-20% of an extruded profile contains the transverse weld (Mahmoodkhani et al., 2014; MI Metals, 2019), which is an elongated solid-state weld that forms between consecutively extruded billets and has a lower strength than surrounding material (Den Bakker et al., 2016). In the case studies, the transverse weld lengths were determined by sectioning, polishing and macro-etching the extruded profiles to reveal the weld line (Section S1.2). Some applications do not require removal of the transverse weld (e.g., concrete screeds (Mag Specialties, 2019)); however, removal is typically mandated by automotive OEMs (Ford Motor Company, 2013). The stop mark is an easy-to-identify blemish on the surface of the profile from where the profile has been pressed against the die exit between ram strokes.

2.2. Intrinsic environmental impacts and costs

Intrinsic environmental impacts and costs (per unit input) were determined from the literature and are presented in Table 2. U.S. electricity impacts were derived using the US Environmental Protection Agency (2020) inventory of GHG emissions and sinks, as well as Argonne National Lab's (2020) Greenhouse gasses, Regulated Emissions, and Energy use in Transportation (GREET) model. The GWP of natural gas (combustion) was determined using the GREET model, and the CED was modeled as Heat Production, Natural Gas, at Industrial Furnace from the ecoinvent 3.1 database. Electricity and natural gas costs were modeled as the average of industrial rates for the Midwest region sampled monthly between 2011 and 2020 (U.S. Bureau of Labor Statistics, 2021a; 2021b). Boron nitride was modeled as a Generic Lubricating Oil, also from the ecoinvent 3.1 database, and costs were determined from commercially available sprays (Zyp Coatings, 2021).

The intrinsic impacts of the aluminum alloy billets were determined using the 'recycled content' method, reflecting a "strong" sustainability perspective where scrap recycling is not assumed to displace primary production like in the 'avoided burden'/'end-of-life' approach (Frischknecht, 2010). For each alloy, the impacts of producing primary aluminum and the alloying elements were determined using the ecoinvent database, which includes the impacts from casting. The billet cost is determined by the cost of primary metal, secondary metal, the Midwest premium (covering the cost of importing and transporting the aluminum into the US (SandP Global Platts, 2019)), and the billet premium (covering the cost of casting aluminum into billets from the ingot form (MI Metals, 2019)). The CES EduPack 2020 database (Granta Design Limited, 2020) was used to estimate the cost of each of the primary alloys. The price of secondary (post-industry) aluminum extrusion scrap

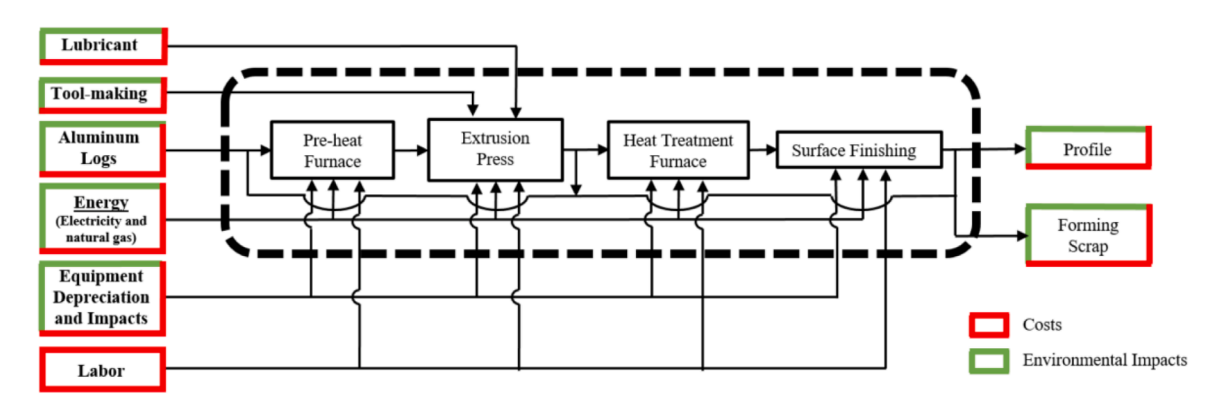


Fig. 2. System boundaries for environmental impact and cost models.

Table 1Descriptions of the solid and hollow case study profiles.

		Casestudy profile	Casestudy profile	
	- at t 1	1	2	
	Profile description ¹	Solid rectangular	Hollow T-slot 80/	
		bar	20 profile	
Profile	Alloy	AA6061	AA6063	
	Alloy yield strength (Y_f)	15	11	
	@ 530 °C (MPa)	1.00	1.00	
	Linear density (kg/m)	1.00	1.38	
	Billet Recycled Content	54	54	
	(%) Billet Cost (\$/kg)	2.52	2.49	
Lubricant	Type	Boron Nitride	Boron Nitride	
Lubricant	Mass (grams/billet)	10	10	
Tooling	Material	H-13 tool steel	H-13 tool steel	
Toomig	Die Type	Solid	Hollow	
	Die Plate Mass (kg)	Blank: 37.8	Blank: 37.8	
	Die Flate Wass (kg)	Removed: 3.1	Removed: 6.6	
		Final: 34.7	Final: 31.2	
	Die Bolster Mass (kg)	Blank: 160.9	Blank: 160.9	
	Die Boister iviass (Rg)	Removed: 11.5	Removed: 11.5	
		Final: 149.4	Final: 149.4	
	Die Lifespan ² (kg)	106,000	20,000	
	Die Cost ³ (\$)	660	1600	
	Dummy Block Mass (kg)	26	26	
	Dummy Block Cost (\$)	1000	1000	
	Dummy Block Lifespan ⁴	680,000	680,000	
	(kg)	000,000	000,000	
	Container Mass (kg)	129	129	
	Container Cost ⁵ (\$)	30,000	30,000	
	Container Lifespan ⁶ (kg)	15 million	15 million	
Equipment	Equipment Mass (kg)	675,000	675,000	
-4P	Equipment Cost ⁷	10	10	
	(\$Million)			
	Equipment Lifespan ⁸ (Mt)	9	9	
	Billet Preheat	530	530	
	Temperature (°C)			
Extrusion	Container Temperature	450	450	
	(°C)			
	Die Temperature (°C)	530	530	
	Ram Speed ⁹ (mm/s)	5.6	3.1	
	Billet Geometry (mm)	Length: 800	Length: 800	
		Diameter: 152	Diameter: 152	
	Extrusion Ratio (ER)	50	30	
	Front-end defect length removed (mm)	3500	2800	
	Billet butt length removed	50.8 (6% of billet	50.8 (6% of billet	
	(mm)	mass)	mass)	
Process	Labor Requirement	4	4	
	(persons)			

Notes: 1. No heat treatment or surface finishing processes were conducted in these case studies. 2. Die life spans range from 20 to 106 t of extruded billet. Dies for extruding simple profiles have longer lifespans. (Thumb Tool and Engineering, 2018). 3. Die costs based on average for solid and short hollow profiles (MI Metals, 2019). Short refers to the depth of the die, a light profile will have a shallow depth as less support is necessary in the die stack. 4. Dummy block lifespan represents 6500 billet pushes (Superior Aluminum, 2019). 5. Container costs for medium sized press, Ø152 to 178 mm (Superior Aluminum, 2020). 6. Container lifespan represents 6 months of production (MI Metals, 2019). 7. Equipment costs encompass a new extrusion press with ancillary equipment (MI Metals, 2019). 8. Equipment lifespan represents 10 years of production (MI Metals, 2019). 9. The ram speed when extruding complex hollow profiles is lower to reduce the required press force and die wear.

was modeled as 87% of primary material (Schlesinger, 2014). The Midwest premium was determined as the average of monthly values in 2020 (SandP, 2019). The billet premium was determined from a range provided by MI Metals (2019).

The embodied environmental impacts of the machinery and the tooling were calculated using the mass of the extrusion equipment (press and billet heating furnace) and tooling (container, dummy block, and die-set) as well as the intrinsic impact values for *Steel Primary Production* and *Chromium Steel Milling, average* obtained from the ecoinvent 3.1

database.

The labor cost is the median wage reported for *U.S. Extruding and Drawing Machine Setters, Operators, and Tenders, Metal and Plastic* (U.S. Bureau of Labor Statistics, 2020a) increased by 45% to account for benefits (U.S. Bureau of Labor Statistics, 2020b).

2.3. Case study results

Electricity was used to preheat the billets and dies in an electric preheat furnace and to power the extrusion press hydraulics, container cartridge heaters, billet butt shear, and auxiliary equipment. The electricity to heat two 40 kg billets to 530 °C over 5.5 h was 48 kWh. Prior to extruding the billets, the press container was heated over 12 h from room temperature to 450 °C, which required 216 kWh of electrical energy. This press preheating energy requirement dwarfs the energy needed to extrude a single billet but in industry this press preheating is only needed after replacement of the press container, a process which requires the press to be cooled but typically only occurs after every ≈ 15 kt of extruded profile (about six months of production (Superior Aluminum, 2019)). Therefore, the environmental impacts and costs of press preheating are negligible when normalized to the functional unit of 1 kg of un-fabricated profile. In industry, billet preheating typically uses continuous natural gas fired furnaces rather than electric ovens; however, the direct energy requirements in the case studies are within the expected range from industry (Figure S2). The billet preheating energy efficiency ($\eta_{preheat}$) is defined as the minimum energy needed to heat the billet $(mc\Delta T)$ divided by the actual, measured, energy delivered to heat the billet, be it electrical energy or thermal energy from combustion of natural gas. In the case studies, $\eta_{preheat}$ was found to be 21%.

Electrical energy is required after press preheating to maintain the container temperature during idling, to operate the hydraulic ram to extrude the billet, and to operate the hydraulic shear to remove the billet butt. Fig. 3 shows the electrical power consumed by the press during the case studies. The active power correlates with the measured ram force: both are at their maximum at the start of the ram stroke and decrease as the ram extrudes the billet and the area between billet and container decreases, reducing frictional resistance. The mean power factor during the case study extrusion process is 0.82. The power factor peaks at 0.96 at the beginning of each ram stroke but drops to 0.39 during idling. Press idling consumes 9-27 kW as the cartridge heaters turn on intermittently. For the case of the solid rectangular bar, over a complete press cycle (600 s, from the start of one ram stroke to the next), 10.15 kWh of electricity was consumed of which 3 kWh was attributable to baseload energy requirements including during idle, 6.79 kWh was the increased energy required to extrude the billet, and 0.36 kWh was attributable to operating the shear.

The extrusion press energy efficiency (η_{press}) is defined as the minimum mechanical energy needed to extrude the billet (the area under the ram force-displacement curve on the right hand side of Fig. 3) divided by the actual electrical energy delivered to extrude a billet (the area under the power-time curve on the right hand side of Fig. 3). In the case studies, η_{press} was 6.3% and 8.2% for the solid and hollow profiles respectively.

The total impacts and costs of the case studies are presented in Fig. 4. It is shown that the aluminum material represents the vast majority of the environmental impacts and costs; e.g., 95.2% of the GWP, 90.7% of the CED and 91.8% of the costs in the solid rectangular profile case study. The material utilization from aluminum log to finished profile was 82% for the solid profile and 81% for the hollow profile. The frontend scrap was the largest source of scrap, closely followed by the billet butt. These process yield losses increase the material impacts and costs, and also the direct energy requirements because extra material must be heated, extruded, and sheared. The relative increase in material costs that results from the yield loss is not as significant as the increase for material CED and GWP because of the significant monetary value of

 Table 2

 Intrinsic environmental impacts and costs.

Input		Density		CED		GWP		Cost
	mean	uncertainty	mean	uncertainty ¹	mean	uncertainty ¹	mean	uncertainty ¹
Energy (I _{energy} , C _{energy})								
Electricity (i _{elec} , c _{elec})		_		J/kWh		CO ₂ e/kWh		\$/kWh
Medium voltage electricity			10.30	0.26	0.41	0.01	0.13	0.077
Gas (i _{gas} , c _{gas})	_		MJ/Therm		kgCO2e/Therm		\$/Therm	
Natural gas			117.90	2.95	5.96	0.15	0.84	0.066
Billet Material (I _{billet} , C _{billet})		kg/m ³]	MJ/kg	k	gCO ₂ e/kg		\$/kg
Primary aluminum (i _{primary} , c _{primary})		Ü		, and the second				· ·
High purity aluminum	2696	_	173.07	4.33	14.80	0.37	2.27	0.13
6061	2713	_	174.88	4.37	14.89	0.37	2.52	0.14
6063	2696	_	174.31	4.36	14.88	0.37	2.49	0.13
6082	2700	_	174.03	4.35	14.82	0.37	2.49	0.13
7075	2796	_	170.50	4.26	14.47	0.36	5.05	0.28
Secondary aluminum (i _{secondary} , c _{secondary} , c _{scrap})								
6XXX extrusion ²	-	-	8.74	0.22	0.74	0.02	2.19	0.12
7XXX extrusion ²	-	-	8.53	0.21	0.72	0.02	4.39	0.24
Billet premium (c _{billet-premium})	-	-	-	-	_	-	0.29	0.01
Midwest premium (c _{midwest-premium})	-	-	-	-	-	-	0.33	0.06
Tooling (I _{tooling})		kg/m ³	1	MJ/kg	k	gCO ₂ e/kg		-
Die Material ($i_{\rm die}$) Tool Steel	7800	-	30.44	0.76	3.25	0.08		
Die machining (i _{removed})	kg/m³		MJ/	kg _{removed}	kgC0	O ₂ e/kg _{removed}		_
Tool Steel	7800	_	111.44	2.79	7.15	0.18		
Lubricant (i _{lubricant} , c _{lubricant})		_	1	MJ/kg	k	gCO ₂ e/kg		\$/kg
Boron Nitride			83.05	2.08	1.13	0.03	50	1.25
Labor (C _{labor})		-		-		_		\$/hr
Operator							26.13	6.90

Notes: 1. All uncertainties are modeled as normal distributions and the numerical value refers to one standard deviation calculated from the sample data reported in the data sources. For example, the primary alloy cost uncertainties were calculated from the range of values reported by the CES Edupack 2020 database. The CED and GWP intrinsic impact uncertainties were derived from ecoinvent's reported 2SD uncertainty values. 2. In these rows, the CED and GWP refer to the environmental impacts of recycled extrusion scrap. The cost, however, refers to the price of the extrusion scrap before recycling. The GWP and CED are assumed to be 5% of their primary values (Blomberg and Söderholm, 2009).

extrusion scrap.

Fig. 4 shows that direct energy and labor requirements also have a significant impact. The labor costs are comparable to the direct energy costs and are higher in the hollow profile case study because of the lower ram and extrudate speed (Table 1). The boron nitride lubricant, press equipment, container, and dummy block tool have a negligible impact (<<1%) on the environment impacts and costs. The relatively short lifespan of the extrusion die (Table 1), however, means that it accounts for approximately 1% of the total cost.

2.4. Global parametric models of extrusion process impacts and costs

2.4.1. Deriving global models

Eqs. (1) and (2) present simple representations of the environmental impact (*I*) and cost (*C*) per kg of un-fabricated profile based on the main contributing factors determined using the case studies.

$$I_{per\ kg\ profile} = \left[I_{log} + I_{tooling} + I_{direct\ energy}\right]_{per\ kg\ profile} \tag{1}$$

$$C_{per\ kg\ profile} = \left[\left(C_{log} - C_{scrap} \right) + C_{tooling} + C_{direct\ energy} + C_{labor} \right]_{per\ kg\ profile}$$
(2)

The impacts and costs of the aluminum metal (I_{log} and C_{log} - C_{scrap}), tooling dies ($I_{tooling}$ and $C_{tooling}$), direct energy requirements ($I_{direct\ energy}$) and $C_{direct\ energy}$), and labor (C_{labor}) are expressed in Eqs. (3 - 9), where α is the overall material yield (0–1) from the DC-cast log to the final profile, R is the recycled content of the log (0–1), $M_{produced}$ is the mass of total finished profile produced (in kg), L_{die} is the lifespan of the extrusion die (in kg of profile produced), M_{die} is the mass of the cast die (in kg), $M_{re-moved}$ is the mass of the cast die that is machined away (in kg) to produce the final die shape, C_{die} is the upfront cost of the extrusion die (in USD), and G_X and E_X are the direct natural gas and electricity requirements needed to perform operation X.

$$I_{\log, per \ kg \ profile} = \frac{R \times i_{secondary-al} + (1 - R) \times i_{primary-al}}{\alpha}$$
(3)

$$\left(C_{\log} - C_{scrap}\right)_{per\ kg\ profile} = \left(\frac{1}{\alpha}\right) \left(R\left(c_{secondary-al} + c_{midwest-prem.} + c_{billet-prem.}\right) + (1-R)\left(c_{primary-al} + c_{midwest-prem.} + c_{billet-prem.}\right)\right) - \left(\frac{1-\alpha}{\alpha}\right)c_{scrap}$$
 (4)

$$I_{tooling, per kg profile} = \frac{\left\lceil \frac{M_{produced}}{L_{die}} \right\rceil (M_{die} \times i_{die} + M_{removed} \times i_{removed})}{M_{produced}}$$
 (5)

$$C_{tooling, per kg profile} = \frac{\left\lceil \frac{M_{produced}}{L_{die}} \right\rceil \times C_{die}}{M_{produced}}$$
 (6)

$$C_{labor,perkgprofile} = \frac{0.96Pw}{60\alpha\lambda V}, where what sunits of \$ / hr, \lambda of kg / m, and Vof m / min.$$
(9)

Eqs. (7 and 8) model the direct energy requirements of a typical extrusion facility where natural gas is used to preheat the billets and in any post extrusion heat treatment. The labor costs (Eq. (9)) are estimated using the number of line and supporting workers (P), the hourly wage (W), and the time to extrude 1 kg profile calculated using the linear density (λ), forming yield, and the expected speed of the extrudate (V) for a given profile.

$$I_{direct\ energy,\ per\ kg\ profile} = i_{gas} \left(G_{preheat} + G_{heat\ treat} + G_{finishing} \right) \ + \ i_{electricity} \left(E_{press} + E_{heat\ treat} + E_{finishing} \right)$$
 (7)

$$C_{direct\ energy,\ per\ kg\ profile} = c_{gas} \left(G_{preheat} + G_{heat\ treat} + G_{finishing}
ight) \ + \ c_{electricity} \left(E_{press} + E_{heat\ treat} + E_{finishing}
ight)$$
 (8)

Practitioners can substitute their own values into the equations where available. Otherwise, the intrinsic impacts and costs shown in Eqs. (1 - 9) (indicated by lowercase letters) are presented in Table 2, and

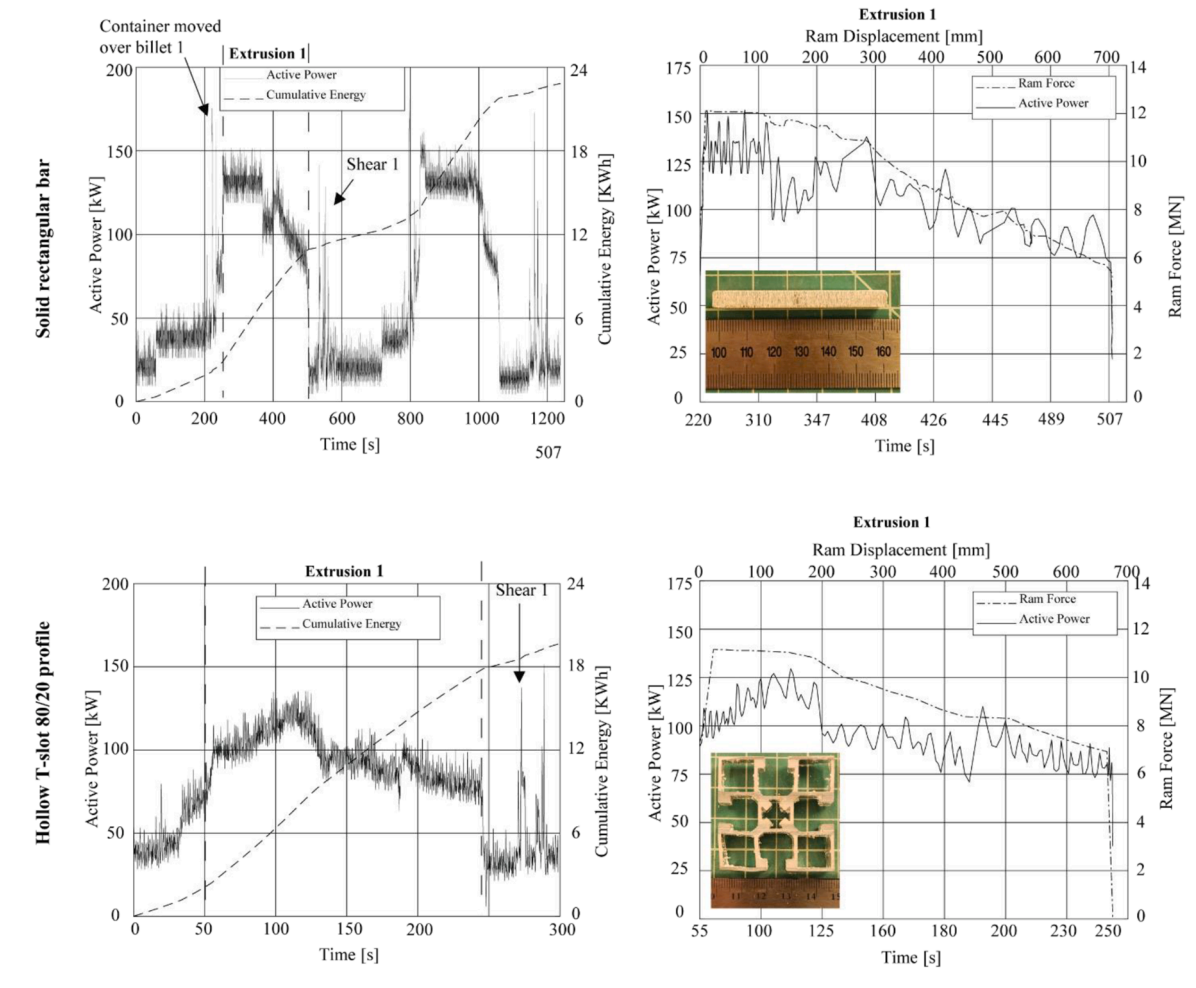


Fig. 3. Active power, cumulative energy and ram force during extrusion of case study profiles.

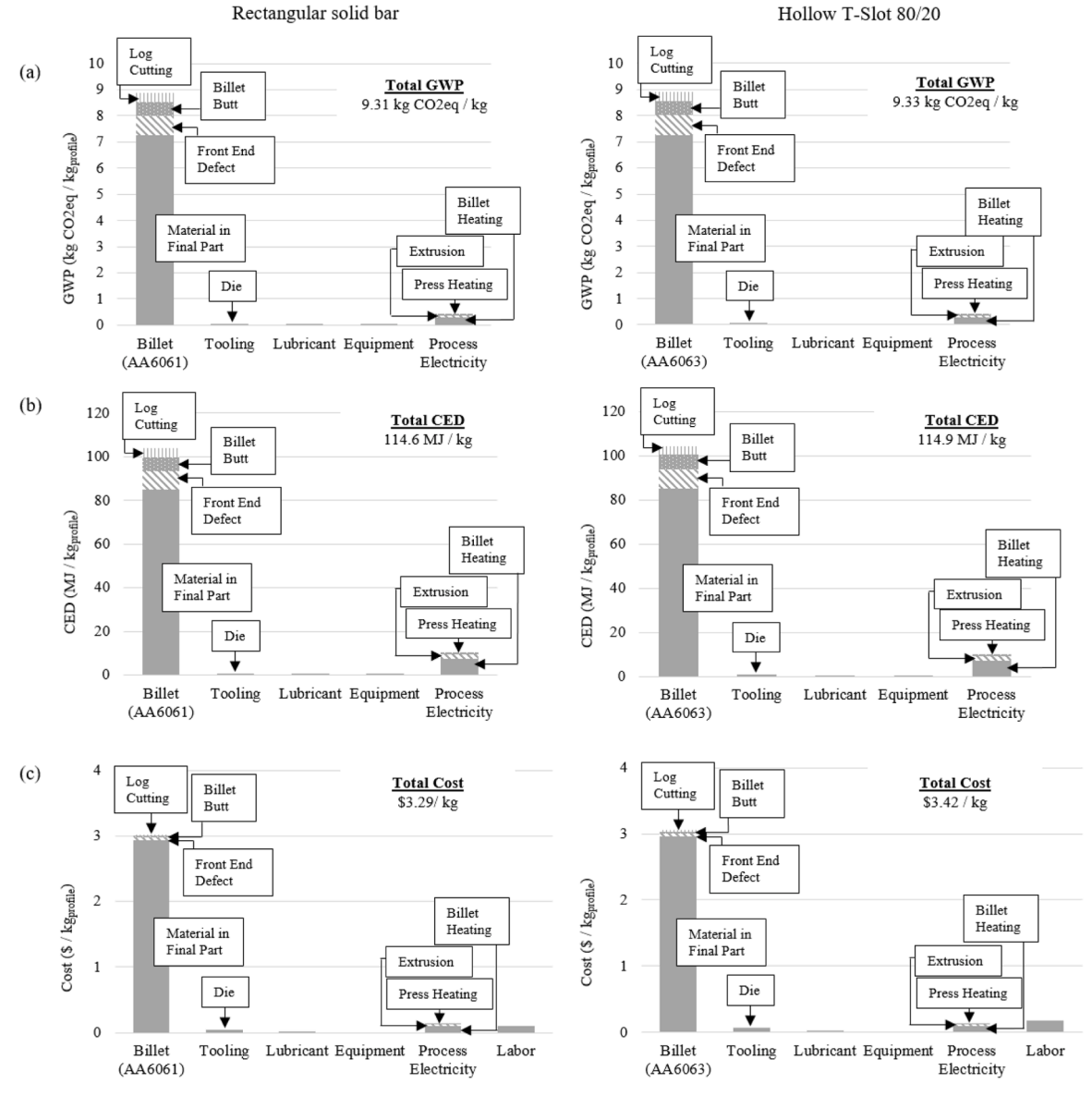


Fig. 4. The (a) Global warming potential (GWP), (b) Cumulative energy demand (CED) and, (c) Costs of the two case study profiles.

representative values for the other life cycle inventory variables (indicated by uppercase letters) are presented in Table 3. Representative inventory values are compiled from industry publications (e.g., European Aluminum Association, 2018), expert interviews (e.g., Superior Aluminum, 2019), and the case study data with physics-based extrapolations. A leading European extruder of automotive profiles provided aggregated direct energy (electricity and gas) data for one year of production (8.7 kt of profiles). The data (provided on the condition of anonymity) is analyzed in S2 and the mean values included in Table 3.

2.4.2. Sensitivity of impacts and costs to key extrusion parameters

The global models were used to determine the effect of key extrusion parameters on environmental impacts and costs: (1) Extrusion press and billet preheating energy efficiency (η_{press} and $\eta_{preheat}$), (2) Forming yield (α), (3) Billet recycled content (R), and (4) Process throughput measured as the extrudate speed (V). Fig. 5 presents the results for extruding a heat treated multi-hollow AA6082 battery tray rail (a typical automotive part) from Ø9" (Ø228.6 mm) billets (see Table S4 for complete details). For clarity, Fig. 5 is constructed just using the nominal inventory and intrinsic impact values reported in Tables 2 and 3. Figure S4 presents the

uncertainty in the results as determined from 100,000 Monte Carlo simulations. Across the parameter space, the uncertainty (one standard deviation) of the GWP and CED is 10.9% and 10.4%, respectively, and the uncertainty of the costs around 11.4%. These error bars mainly reflect the uncertainty in the intrinsic billet impacts (Table 2) and the billet and wage costs.

At the current industry standard, for each 1 kg of battery tray profile, 0.021 therms of natural gas is used to preheat 1.31 kg of billet which is then extruded using 0.46 kWh of electricity. This conforms to the range of aggregated direct energy values provided by the European automotive extruder (Figure S2). Fig. 5a shows that increasing the extrusion press and billet preheating energy efficiency can significantly lower the environmental impacts but cost savings are more modest: \approx 6% reduction in CED and <2% reduction in costs for 100% energy efficiency. However, Fig. 5b shows that the greatest reductions in environmental impacts are from increasing the process forming yield and the billet recycled content. A 10% increase in the forming yield from 76.3% to 83.9% results in GWP, CED and costs being reduced by 9.03%, 8.97% and 3.17% respectively. A 10% increase in recycled content reduces the environmental impacts by \approx 10% but the costs by only \approx 0.7%. Fig. 5c

 $\begin{tabular}{ll} \textbf{Table 3}\\ Extrusion characteristics for predictive models (S2). Uncertainties correspond to 1 standard deviation and are modeled as normal distributions calculated from the respective data sources. \end{tabular}$

the respective data sources.		
	Nominal value	Uncertainty
Recycled content, R %	54	10% of
		nominal
Dan	76.0	value
Process yield, α %	76.3	10% of nominal
		value
Extrusion press energy	7.25	10% of
efficiency, η_{press} %		nominal
F		value
Billet preheat energy	21	10% of
efficiency, $\eta_{preheat}$ %		nominal
Die \cos^1 , C_{die} \$	$10338.5 \times CCD + 234.2 \times P_{tot} \times S$	value 10% of
Die Cost , C _{die} \$	$10336.3 \times CCD + 234.2 \times P_{tot} \times 3$	nominal
		value
Die Lifespan² (average),	63,000	6000
L_{die} kg _{profile}		
Hollow die	20,000	6000
Solid Die	106,000	6000
Mass die ³ , M _{die} kg	$(3.81~ imes10^{(-8)}) imes ho_{ ext{tool steel}} imes\pi imes$	10% of
	$(2D_{container})^2$	nominal
Mass romand (salid)4	$0.15M_{die}$	value 10% of
Mass removed (solid) ⁴ , $M_{removed}$ kg	0.15IVI _{die}	nominal
Wiremoved Kg		value
Mass removed (hollow)4,	$0.3M_{die}$	10% of
$M_{removed}$ kg		nominal
		value
Number of workers ⁵ , P	4	0.5
Speed of the extrudate, V		10% of
m/min.	27	nominal
(AA6061) ⁶ (AA6063) ⁶	45 14.5	value
(AA6082) ⁷	1.6	
(AA7075) ⁶		
Preheat gas ⁸ , G _{preheat}	(0.96)	10% of
therms/kg _{billet}	$\left(\frac{}{\alpha}\right)^{\times}$	nominal
	$\left(rac{900 imes (T_{billet} - T_{ambient})}{\eta_{preheat}} ight) imes$	value
	$\left(\frac{1}{29.3\times3600000}\right)$	
	(29.3 × 3600000)	
	or European collaborator average:	
	European collaborator average: 0.014	
Heat treat gas, Gheat treat	European collaborator average:	10% of
therms/kg _{profile}	0.001	nominal
		value
Finishing gas, Gfinishing	European collaborator average:	10% of
therms/kg _{profile}	0.022	nominal
		value
Heat treat electricity,	European collaborator average:	10% of
$E_{heat\ treat}\ kWh/kg_{profile}$	0.045	nominal
Finishing electricity,	European collaborator average:	value 10% of
E _{finishing} kWh/kg _{profile}	0.960	nominal
-juising		value
Press electrical energy,	$\frac{0.96}{3600000 \times \alpha} \times \frac{e_{mech}}{\eta_{press}}$	10% of
E_{press} kWh/kg _{profile}	$\overline{3600000 \times \alpha}^{\times} \overline{\eta_{press}}$	nominal
	or	value
	European collaborator average:	
	0.56	
Minimum mechanical	$L_{billet} \frac{\pi D_{billet}^2}{4} K_x Y_f \left(ln(ER) \right. + $	10% of
energy to extrude the	_ `	nominal
billet ⁹ , E_{mech} MJ	$\left(\frac{L_{billet}}{D}\right) \times 10^{-9}$	value
Minimum mechanical	$\left(\frac{L_{billet}}{D_{billet}}\right) \times 10^{-9}$ $\left(\frac{1}{\rho}K_xY_f\left(ln(ER) + \frac{L_{billet}}{D_{billet}}\right)\right)$	10% of
energy to extrude the	$\frac{-K_x Y_f}{\rho} \left(ln(ER) + \frac{\sigma_{billet}}{D_{billet}} \right)$	nominal
billet per kg of billet,	,	value
e_{mech} MJ/kg		
Shape Factor ^{1,10} , K_x	$0.98 + 0.02 igg(rac{P_{tot}}{C_{eq}}igg)^{2.25}$	10% of
	$0.50 \pm 0.02 \left(\frac{C_{eq}}{C_{eq}} \right)$	nominal
		value

Notes: 1. Die cost model from Nieto (2010) based on an empirical multivariate regression analysis performed on quotes obtained from toolmakers and covering a wide range of die designs. The circumscribing circle diameter (CCD, measured in mm) describes the minimum circle diameter that fully encompasses the profile, the total perimeter (P_{tot} , measured in mm) is the total perimeter of the profile cross section (sum of internal and external perimeters) and the shape factor (S) describes the type of die, S = 1 for solid profiles, S = 2 for semi-hollow profiles with at least one partially enclosed void, S = 2 for class 1 hollows (with a void of 25.4 mm or greater) and class 2 hollows (any hollow profile other than class 1 that does not exceed CCD = 127 mm), and $S = 1 + N_{voids}$, where N_{voids} is the number of voids, for class 3 hollows (all hollow profiles that are not class 1 or class 2). 2. Based on discussions with TTE (2018). Extrusion dies are typically made from H13 tool steel, 3. Based on discussions with TTE (2018): Die diameter is twice container diameter and a 6'' die thickness is typical. $D_{container}$ is the diameter of the extrusion press container in mm. 4. Based on discussions with TTE (2018). 5. Based on discussions with Kaiser Aluminum (2020). 6. Data from Misiolek and Kelly (2005). 7. Data from Tomczyk (2019). 8. Specific heat capacity of aluminum = 900 J/Kg °C; Conversion from J to therms = $\frac{1}{29.3~\times~3,600,000}\text{;}$ default $T_{billet}=450~^{\circ}\text{C}$ and $T_{ambient}=20~^{\circ}\text{C}.$ 9. The mechanical energy (e_{mech}) is calculated using a lower bound slab analysis to estimate the necessary extrusion force at the beginning and end of the press stroke and integrating over the ram stroke distance (see Section S3.1). Billet dimensions are measured in mm. Yf is the aluminum yield stress at the extrusion temperature measured in MPa (see Table S5 for example data). 10. C_{eq} (in mm) is the equivalent circumference, or the circumference of a circle with an area equal to the profile cross-section. 11. In Eqs. (1-9) and Table 3, the "0.96" coefficient accounts for the log-to-billet cutting yield loss of 4%.

shows the great increase in cost when using extrusion speeds similar to those used for AA7075 due to a low throughput.

3. Material flow analysis of the North American extrusion industry

The analysis presented in Section 2.4 shows that increasing material efficiency (process yields and billet recycled contents) will have the greatest effect on reducing the environmental impacts and costs of the aluminum extrusion industry; however, no detailed MFAs exist showing the markets (e.g., alloys, section shapes, and applications) in which material efficiency efforts should focus. In this section, an MFA of the North American (U.S. and Canada) aluminum extrusion industry in 2018 is derived; North America in 2018 is the region and most recent year for which extensive data is available.

3.1. Constructing a map of aluminum extrusion flows

A wireframe map representation of the MFA (Figure S5) was produced based on existing industry analyses (e.g., Mulholland, 2016) and refined based on industry interviews. The wireframe map defines the key processes along the supply chain and the existence or absence of material flows between the different processes; e.g., the existence of a flow of imported ingots into North American secondary billet production. At each step along the supply chain, data (\hat{x}) were collected on the material origin, mass of material processed, process yield, alloy, and destination/application. Over 100 MFA data records (Table S17) were collected from industry associations (e.g., International Aluminum Institute (2021)), national and international statistical agencies (e.g., UN Comtrade data (2018)), publicly available industry databases (e.g., Norsk Hydro (2020a, 2020b)), academic and gray literature, and 100 semi-structured interviews with industry experts from each part of the supply chain: billet production, extrusion, recycling, fabrication, and end-use. Table S15 summarizes the main data sources.

3.2. MFA data reconciliation (S4)

As is common in MFA, data records on many of the MFA parameters are either missing or inconsistent; i.e., different data sources record

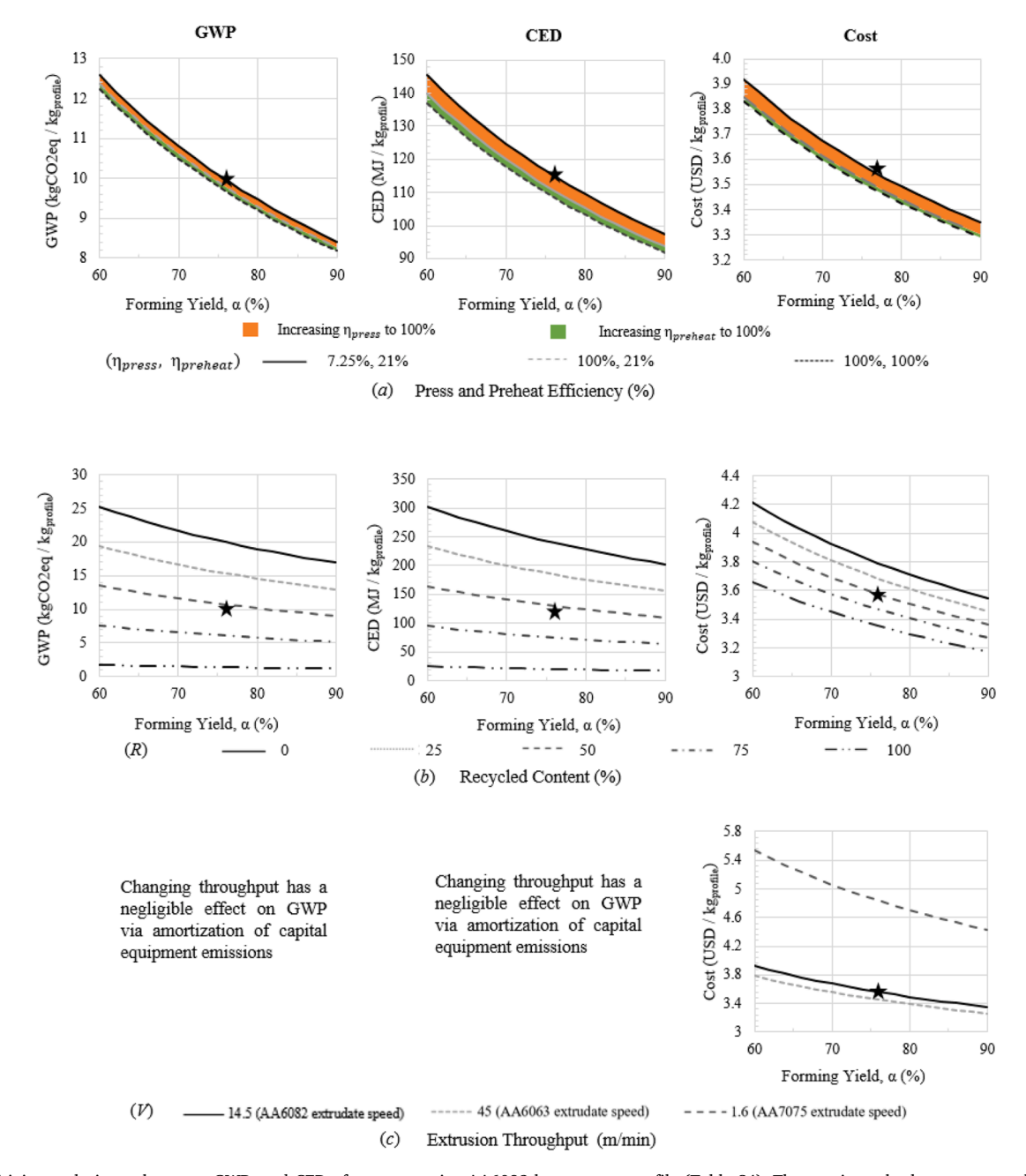


Fig. 5. Sensitivity analysis on the costs, GWP, and CED of an automotive AA6082 battery tray profile (Table S4). The star in each plot represents the current industry standard.

different (contradictory) values for the same MFA parameter or data records on neighboring MFA parameters suggest a violation of the conservation of mass. For example, no reports were found quantifying the annual production volume of primary and secondary billet by alloy in North America in 2018. Elsewhere in the data collection process, the reported annual production of extrusions from Bertram et al. (2017) in conjunction with the reported fabrication process yield from Cullen and Allwood (2013) suggest that 2.65 Mt of fabricated extrusions were produced in 2018, which is inconsistent with the 2.28 Mt of fabricated extrusions reported by Sattlethight (2019). A set of internally consistent, mass-balanced MFA parameters (x_i) is generated using an adaptation of Zhu et al's (2019) nonlinear least squares data reconciliation method, which itself is developed from earlier work by Kopec et al. (2016). Zhu et al.'s method is used because it is easily updatable, can handle a plethora of data types (e.g., process yield ratios), and presents a consistent method for assigning a confidence score ($\varphi_{i,i}$: 0–1) to each

collected data record. In the reconciliation, the objective function presented in Eq. (10) is minimized subject to conservation of mass constraints. $r_{i,j}$ are the normalized residuals between the collected data (\widehat{x}_{ij}) and reconciled data (x_i) . J_i is the total number of empirical data records collected for each MFA parameter, i. For each data record, the confidence score $(\varphi_{i,j})$ was determined based on the alignment of the data record with the desired coverage (1–4; 1 = single case study; 4 = data from >50% of industry), frequency (1–4; 1 = single data point; 4 = at least monthly data collection), and spatial boundary of the source (1–4; 1 = data scaled from Global data and/or a different industry; 4 = data from only North American extrusion industry) (see Table S14); e.g., the AEC's annual end-use survey has a confidence score of 0.917 (coverage score of 4/4, frequency score of 3/4, spatial boundary score of 4/4, for a total score of 11/12 = 0.917). Table S17 presents a complete list of the collected data records $(\widehat{x_i})$ and the corresponding confidence scores $(\varphi_{i,j})$

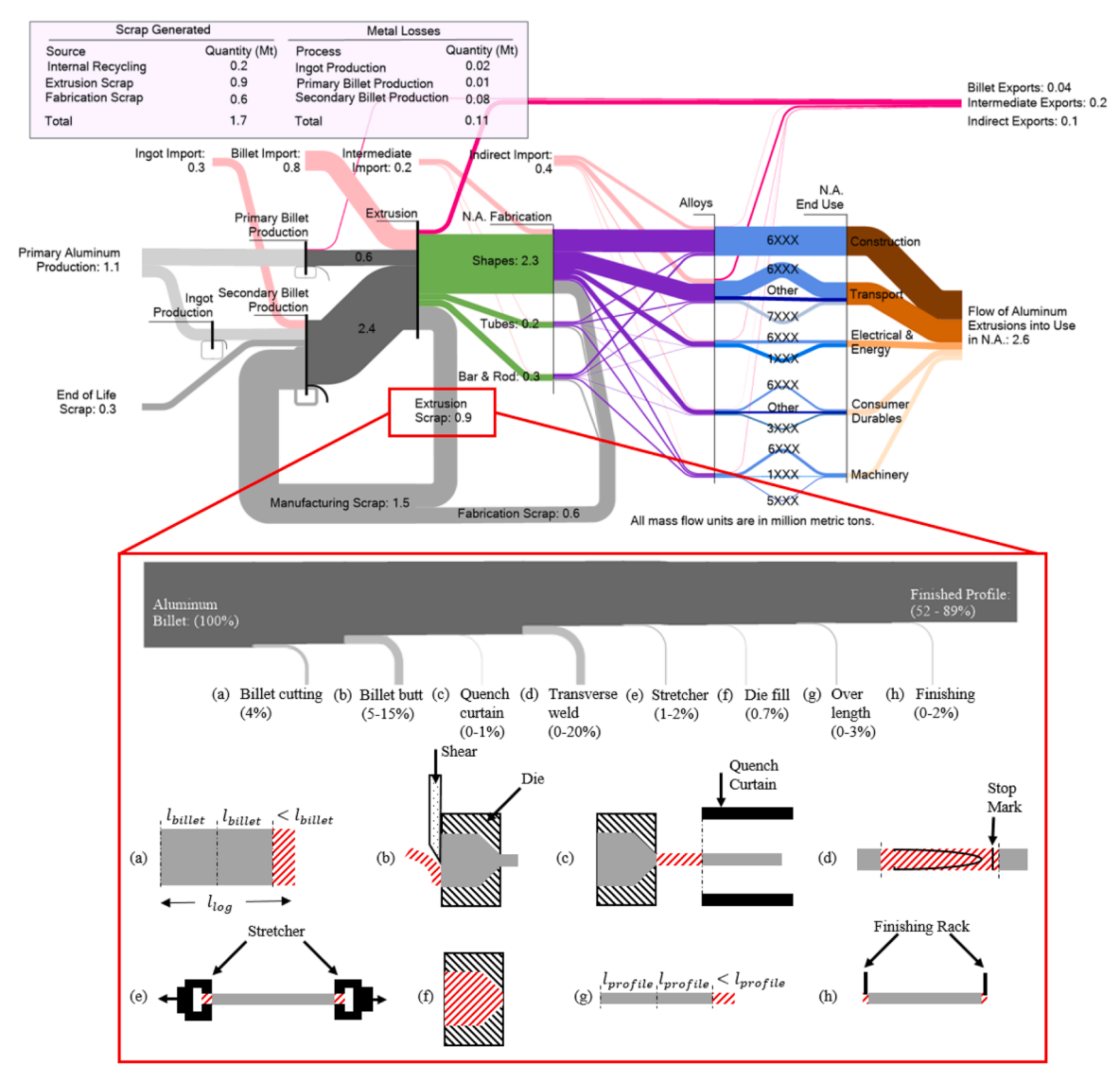


Fig. 6. Top: Sankey diagram representation of the material flow of aluminum extrusions in North America (N.A.: U.S. and Canada) in 2018 (Note: Aluminum alloying is done during billet production and it is only placed after extrusion here to clearly show the flow of fabricated profiles). Bottom: The flow of aluminum for a typical extrusion from DC cast log to unfabricated aluminum profile showing the range of scrap generated at each stage of the extrusion process as a red hashed area.

used in this MFA data reconciliation.

Minimize:
$$\sum_{i=1}^{I} \frac{\sum_{j=1}^{J_{i}} \phi_{i,j} \times (r_{i,j})^{2}}{J_{i}} \text{ where } r_{i,j} = \frac{J_{i}(x_{i} - \widehat{x}_{ij})}{\sum_{j=1}^{J} \widehat{x}_{ij}}$$
(10)

In order to increase the likelihood of convergence to a near global optimum solution, the initial set of values used in the nonlinear optimization is equal to the weighted mean (by confidence score) of all data records for each MFA parameter. If no recorded data is available, initial values are calculated using simple mass balance. The optimization was implemented with Matlab's fmincon algorithm using the "interior-point" method. It took 201 iterations for the objective function to converge (Figure S7): 20 min on an AMD Ryzen 5 2600 CPU, 3.40 GHz with 16 GB of 3200 MHz RAM. The optimization achieved mass balance after an initial maximum constraint violation of 0.51 Mt (corresponding to a discrepancy between reported billet consumption, extrusion production and yield rate) and reduced the objective function by 42% from a maximum of 0.024 during mass balancing to 0.014 at convergence (Figure S7). The code and data used for this MFA reconciliation is available for download (see S6.3).

3.3. MFA results

The estimated 2018 North American aluminum extrusion material flow is shown in Fig. 6 as a Sankey diagram, where the width of each line is proportional to the mass flow. The light gray lines represent scrap flows and the black lines represent system losses (e.g., dross generation).

In 2018, North America consumed approximately 2.6 Mt of fabricated aluminum profiles embedded within end-use products. The domestic North American industry consisted of around 500 extrusion presses operated by approximately 130 extrusion companies (Consulting Collaborative, 2017) that produced a total of 2.9 Mt of un-fabricated profile (0.2 Mt for export) from 3.8 Mt of billet (76% mean process yield, excluding log-to-billet cutting) with over half (52%) of production from just five large companies: Hydro, Kaiser, Bonnell, UMEX and Extrudex (Consulting Collaborative, 2017). A further 20% of the aluminum was scrapped during fabrication into finished products. At all points along the supply chain, North America was a net importer of ingots, billets, intermediate (un-fabricated) profiles, and indirect (finished) goods.

Fig. 6 shows that despite the dominance of secondary billet production in North America, relatively little end-of-life (post-consumer) scrap is used. Instead, secondary billet feedstock is largely

manufacturing scrap and primary ingot. Extrusion process scrap is largely closed loop recycled into extrusion billet; however, secondary billet production creates more internal runaround scrap as well as $\approx 3\%$ losses to dross generation. The North American extrusion industry produces many thousands of different profile shapes; however, these shapes can be categorized under three broad banners: (1) solid profile (and largely commodity) rod and bar, (2) simple tubes, and (3) complex shapes that account for 82% of the market. Fig. 6 shows that 6xxx series alloys dominate production and that the transport sector end use demand is comparable to the construction industry. Figure S8 shows the flow of different alloys into different construction and transport subcategories. Commercial façade is the single greatest destination for extrusions across construction and transport, and the destination of transport extrusions is evenly split between cars and light trucks, semis and trailers, and 'other' (e.g., truck, bus, RV, rail). More extrusions are used in electric vehicles than any other type of vehicle (Dinsmore, 2018). Applications include simple cylindrical rods used as machining stock (Norsk Hydro, 2020b), to roof bows (e.g., Tesla Model S (Design News Staff, 2014)), battery housings (e.g., in the Ford Mustang Mach-E EV (Page, 2020)), and trim and crash management systems (Ducker

Fig. 6 (bottom) shows the contribution of various process yield losses to the estimated 0.9 Mt of extrusion process scrap. These additional yield losses (beyond billet log cutting, billet butt, and front-end defect scrap) are often absent depending on the context (alloy, desired surface finish etc.). A quench box is used when the extruded profile is made from a heat treatable aluminum alloy (e.g., AA6082) that requires rapid water spray cooling in order to create a supersaturated solid solution (SSSS) in preparation for precipitation hardening. There is often a gap of approximately 1.2 m between the exit of the die and the start of the quench curtain due to imperfect integration of the press and quench box machine designs (Fig. 6c). This gap results in the last section of extruded billet experiencing natural air cooling as it is left stationary between the die and quench curtain while the ram is retracted, the billet butt sheared, and a new billet loaded into the container. Natural cooling prevents the creation of a suitable SSSS that can be subsequently age hardened; therefore, this section of material between the die and the quench curtain is scrapped. After extrusion, lengths of profile equal to the run-out table length are typically straightened using a stretcher machine that grips the ends of the profile and imposes a 1-3% tensile elongation. The material squeezed by the grippers is often deformed and scrapped. After a production run is finished, the extrusion die is allowed to cool and is cleaned before future use. Billet material entrapped within the die at the end of a production run is scrapped. When sectioning the stretched profile into desired lengths there are often leftover lengths of material that are discarded as scrap. Finally, scrap may also be created as a result of the finishing process (e.g., anodizing) when profiles are loaded on racks for finishing but where material in contact with the racks receives a poor finish and is subsequently trimmed.

A formal uncertainty analysis on the results presented in Fig. 6 (top) is not possible because extrusion production statistics are not published with error bands. This is a common problem in MFA (Cullen et al., 2012). The uncertainty is mitigated in this study, as much as is possible, through the use of trustworthy data sources wherever possible, confidence scores to weight the data records, and a mass-balancing data reconciliation of the collected MFA data records. The final reconciliation result is presented to the nearest 100,000 tons, or 1 significant figure in the case of values below 100,000 tons. Figure S10 shows the average residual for the MFA flow variables, and indicates the level of discrepancy between the final MFA result and the initial data records. The largest residual is close to 10% and originates from the difference between the reconciled value for the total production of extruded profiles fabricated in North America (2.7 Mt) compared to a value of 3 Mt from Sattlethight (2019). Despite the uncertainty in the final results, the global MFA presents an estimate of the North American extrusion industry that can be used to inform decision making in industry and

academia.

4. Discussion

This work presents a comprehensive environmental analysis of aluminum extrusion including electrical energy measurements, aggregated industry data, predictive models, and material flow analyses, with the opportunities to reduce impacts compared to the likely effect on costs. Uncertainties in the numerical results are significant (Section 2.4, S3.3) but these have not prevented the influential parameters from being identified. The global models show that there is significant scope for increasing the extrusion press and preheat energy efficiency; however, increasing the material efficiency (process yield and billet recycled content) of the extrusion process represents the greatest opportunity to reduce both the environmental impacts and the costs (Fig. 5).

4.1. Reducing billet preheating and extrusion press energy requirements

The extrusion process is energy-intensive: the primary energy of billet preheating and extrusion is greater than for aluminum remelting in recycling (Figs. 4 and 5 versus Table 2). This article has found significant scope for improving the energy efficiency of the extrusion process. The case study data are used to quantify an energy efficiency metric for billet preheating ($\eta_{preheat}$) and for the press (η_{press}) at 21% and \approx 7.25% respectively. In targeting billet preheat efficiency improvements, a U.S. Department of Energy study (2003) found that replacing the burners in furnaces with new, more efficient burners could decrease natural gas consumption by 30–40% with a payback period of less than 1 year. These higher efficiency burners include self-regenerative burners that recycle the hot exhaust air as pre-heated combustion air; Wünning (2007) found that self-regenerative burners can generate energy savings of more than 20%.

One reason for the low extrusion press efficiency is that the full power capacity of the press is sized for generating the maximum forming force; however, these peak forces are only required for a small fraction of the cycle time at the beginning of the press stroke (see Fig. 3) leading to low average and minimum power factors and high line currents, which increase line and transformer energy losses (Cooper et al., 2017). Furthermore, in conventional hydraulic presses all the main pumps are operating continuously even during idling (SMS Group, 2020). In a recent study (Schreiber et al., 2016), Danieli Breda (an extrusion press manufacturer) measured 5-20% extrusion press energy savings when switching from classic servo-piloted variable displacement pumps equipped with fixed-speed motors to variable displacement pumps and variable speed motors controlled by a variable frequency drive. As described by Cooper et al. (2017), these devices save energy by slowing (or stopping) a motor to match light loads and as energy use is proportional to the cube of the flow rate in the hydraulic system, small reductions in flow can yield disproportionately large energy savings (Nadel et al., 2002). Elsewhere, a recent aluminum extrusion plant retrofit in the Netherlands with a start-stop system led to a 10% reduction in the electrical energy consumption of the main press drives (SMS Group, 2020). Within North America, Superior Aluminum (2019) saw a 2-year payback period in energy savings following a pump and motor replacement in several of their presses. A greater number of new presses now have hybrid drives where hydraulics are used to generate the forming force but all other press movements are delivered through servo drives (Anacker, 2020; Macedonio, 2021). Another option for reducing the press' direct energy requirements is to reduce the mechanical energy needed to extrude the profile (e_{mech} , Table 3) by optimizing the billet geometry. Increasing the billet (and container) diameter while maintaining the billet volume will reduce the mechanical energy requirement but can increase the maximum ram force requirement and is constrained by the force limit of the press (see S7 for analysis and experimental evidence).

4.2. Opportunities for material efficiency

The reconciled MFA (Section 3) suggests that the average recycled content of profiles produced in North America is around 50% and that 40% of all aluminum cast into extrusion billets is scrapped before being used in a fabricated product. Increasing the billet recycled content would result in a significant decrease in environmental impacts (see Fig. 5). Manufacturing scrap produced in the extrusion industry is already (typically) closed-loop recycled back into extrusion billets but there are opportunities to increase recovery of end-of-life extrusion scrap, particularly from vehicles which contain increasing quantities of aluminum extrusions but which are currently shredded at end-of-life with contaminated mixed alloy aluminum scrap exported or downgraded as zorba/twitch (Zhu et al., 2021). Recovery of automotive extrusions will require greater disassembly or automated separation of scrapped vehicle materials. Currently, these activities are prohibitively expensive but might be aided in the future by a greater focus in vehicle design for recycling and emerging cheap and high throughput alloy separation recycling technologies (Zhu et al., 2021). Another barrier to increasing billet recycled contents is that extruders often exclusively use primary billet for safety-critical and esthetic parts; e.g., wing spars in the aerospace industry (Boeing, 2020). Greater research into guaranteeing profile properties from secondary billet could prove fruitful here. Elsewhere, the embodied impacts for non-critical parts could be further reduced if conventional cast billets were substituted with chip billets of compacted machining swarf manufacturing scrap. Numerous researchers have studied this solid-state recycling technology for a decade and have shown that the scrap fragments weld together in the solid-state as they pass through the extrusion die, creating profiles with mechanical properties similar to those produced from conventional billets (Cooper et al., 2018; Tekkaya et al., 2009; Cooper, 2013).

Fig. 6 shows that the main sources of manufacturing scrap are extrusion process scrap (dominated by the billet log cutting scrap, the sheared billet butt scrap, and the transverse weld scrap), and fabrication scrap. There's the potential to employ billet selection and cutting optimization algorithms that help to minimize billet log cutting scrap (Masri and Warburton, 1998), particularly at smaller extruders where this technology is typically still not used today. Elsewhere, researchers have found modest reductions in the transverse weld length (up to \sim 15%) can be achieved by optimization of the ram velocity, ram-billet lubrication, and port-hole die geometry (Hatzenbichler and Buchmayr, 2010; Zhang et al., 2017). Recently, Oberhausen et al. (2021) showed preliminary evidence that novel dummy block and billet geometries could be used to control the flow of the billet-on-billet interface through the extrusion die and result in >50% reductions in transverse weld lengths, at least for simple profiles such as the rod and bar market revealed in Fig. 6. For non-aesthetic profiles, there may also be the opportunity to utilize the profile between the stop mark and the "nose" of the transverse weld (0.15 m and 1 m in the solid and hollow profile case studies respectively) if this section is not already being used to grip the profile for stretching. Elsewhere, quench curtain scrap could be minimized by careful integration of equipment to minimize the die to quench curtain gap. New grippers and racks could also be designed to minimize stretcher and finishing scrap. Finally, profile fabrication yields might be increased through greater supply chain coordination between extruders and manufacturers so that correct lengths are produced directly at the extrusion plant. The development of smart connected manufacturing systems as part of industry 4.0 might enable this efficiency.

4.3. Scale of the opportunity and industry trends

The global parametric models (Section 2.4) are used to estimate the potential environmental and economic benefits of increasing the extrusion industry's material efficiency. For a typical North American extruder, producing 20 kt of final profile per year, a 10% increase in the material efficiency of the extrusion forming process (increasing from an

average of 76.3% to 83.9%) would result in annual savings of 18 kt.CO₂ eq and \$2.2 million. These emissions savings originate from avoiding the production and processing of billet material with a recycled content of 54%. Calculating the benefits of achieving higher process yields at a larger scale (e.g., nationally) is more complicated. On the one hand, an attributional approach can continue to be used to calculate the savings associated with avoiding production and processing of billet material with a recycled content of 54%. On the other hand, a consequential approach considers that a consequence of achieving higher process yields at a larger scale may be that the billet recycled content decreases as there will be less process scrap available for recycling (see Fig. 6). At this larger scale, the consequential approach implies that the effect of higher process yields is to reduce the quantity of material that must be processed through the extrusion process and to shrink the return loop of scrap metal to billet production; therefore, the liquid metal production displaced due to higher process yields has a recycled content of around 96%, with 4% primary production accounting for metal losses during scrap remelting (Boin and Bertram, 2005). Subsequently, for North America (annual production: 2.6 Mt), it is estimated that a 10% increase in the material efficiency of the extrusion forming process would translate to annual savings of between \$270 million and 0.5 Mt.CO_{2.eq} (consequential approach) and \$311 million and 2.3 Mt.CO_{2.eq} (attributional approach). Finally, the global industry (annual production: 28 Mt) would save between \$2.9 billion and 5.4 Mt.CO_{2.eq} (consequential approach) and \$3.35 billion and 25.2 Mt.CO_{2.eq} (attributional approach). Despite the decrease in scrap availability due to higher process yields, the attributional savings could be achieved if the billet material recycled content were maintained through increased recycling of post-consumer scrap.

Current industry trends will only exacerbate the need to improve the extrusion industry's material efficiency. The MFA (Fig. 6) shows that the extrusion of complex shape 6xxx profiles for the transport sector already accounts for 26% of extrusion demand. This market share is set to grow and is a sector where removal of the transverse weld scrap is typically mandated by the OEM. The industry interviews conducted for this study revealed a trend towards more complex cross-sections, thinner walls, and higher strength (7xxx series) profiles for light weighting in the automotive market. However, deployment of these profiles, which would reduce transport use phase emissions, is hindered by the reduced throughput from extruding thinner and harder material profiles and the increased reject rate from excessive distortion when quenching complex multi-cavity profiles. Fig. 5c shows the large cost increase that accompanies the slower 7xxx alloy throughput. Increasing process yields could counter the effect of reduced extrusion speeds on the throughput and the inflated material costs of rejected parts by reducing the process time that is effectively dedicated to producing scrap.

5. Conclusion

In this work, extrusion cost and environmental impact models have been derived and a sensitivity analysis performed to identify the key inputs. The opportunities that have been identified include: (1) Reduction of the billet preheating energy requirements through the implementation of high efficiency burners, (2) Reduction of extrusion press energy requirements through variable frequency drive hydraulic pumps, (3) Increased billet (post-consumer scrap) recycled content in noncritical applications, and (4) Improved material efficiency through increased forming and fabrication yield rates. An MFA of the 2018 North American (U.S. and Canada) extrusion industry is used to evaluate the scope for material efficiency and subsequently the opportunities and barriers to increased process yields are discussed.

CRediT authorship contribution statement

Gregory Oberhausen: Formal analysis, Methodology, Software, Writing – original draft, Writing – review & editing. **Yongxian Zhu:**

Software, Writing – review & editing. **Daniel R. Cooper:** Conceptualization, Formal analysis, Methodology, Writing – original draft, Writing – review & editing, Supervision, Project administration.

Declaration of Competing Interest

The authors declare that they have no known competing financial interests or personal relationships that could have appeared to influence the work reported in this paper.

Acknowledgements

Thank you to the LIFT Manufacturing USA institute for their help with the case studies. Thank you to all the companies that shared their data and knowledge. The authors were supported by the Michigan Translational Research and Commercialization (MTRAC) program and NSF I-Corps and PFI grants.

Supplementary materials

Supplementary material associated with this article can be found, in the online version, at doi:10.1016/j.resconrec.2021.106120.

References

- AEC, 2021. Aluminum Extrusion Backgrounder [WWW Document]. URL https://cdn. ymaws.com/www.aec.org/resource/resmgr/PDFs/BackgrounderAlExt.pdf (accessed 6.9.21).
- Allwood, J.M., Cullen, J.M., Carruth, M.A., Cooper, D.R., McBrien, M., Milford, R.L., Moynihan, M.C., Patel, A.C., 2012. Sustainable Materials - with Both Eyes Open: Future Buildings, Vehicles, Products and Equipment. Sustainable Materials - with Both Eyes Open: Future Buildings, Vehicles, Products and Equipment, 1st ed. UIT Cambridge Ltd., Cambridge, UK.
- Allwood, J.M., Cullen, J.M., Milford, R.L., 2010. Options for achieving a 50% cut in industrial carbon emissions by 2050. Environ. Sci. Technol. 44, 1888–1894. https:// doi.org/10.1021/es902909k.
- Anacker, S., 2020. Higher productivity and energy efficiency with hybrid drive concept for aluminum extrusion presses [WWW Document]. Steel Grips. URL https://www. steel-grips.com/10-news/336-higher-productivity-and-energy-efficiency-with-hybr id-drive-concept-for-aluminum-extrusion-presses (accessed 6.9.21).
- Argonne National Laboratory, 2020. GREET Model [WWW Document]. URL http://greet.es.anl.gov (accessed 7.28.21).
- Ashby, M.F., 2020. Materials and the Environment. Materials and the Environment, 3rd ed. Elsevier, Oxford, doi:10.1016/B978-0-12-821521-0.15001.
- BBC, 2010. Villagers Despair in Hungary's red Wasteland [WWW Document]. BBC News.

 URL. https://www.bbc.com/news/world-europe-11523573 (accessed 10.30.21).
- Bertram, M., Ramkumar, S., Rechberger, H., Rombach, G., Bayliss, C., Martchek, K.J., Müller, D.B., Liu, G., 2017. A regionally-linked, dynamic material flow modelling tool for rolled, extruded and cast aluminium products. Resour. Conserv. Recycl. 125, 48–69. https://doi.org/10.1016/j.resconrec.2017.05.014.
- Billy, R., 2012. Material Flow Analysis of Extruded Aluminium in French Buildings. Material Flow Analysis of Extruded Aluminium in French Buildings. Norwegian University of Science and Technology.
- Blomberg, J., Söderholm, P., 2009. The economics of secondary aluminium supply: an econometric analysis based on European data. Resour. Conserv. Recycl. 53, 455–463. https://doi.org/10.1016/j.resconrec.2009.03.001.
- Boeing, 2020. Boeing roundtable discussion.
- Boin, U.M.J., Bertram, M., 2005. Melting standardized aluminum scrap : a mass balance model for Europe. J. Miner. 26–33. https://doi.org/10.1007/s11837-005-0164-4.
- Cann, J.L., De Luca, A., Dunand, D.C., Dye, D., Miracle, D.B., Oh, H.S., Olivetti, E.A., Pollock, T.M., Poole, W.J., Yang, R., Tasan, C.C., 2020. Sustainability through alloy design: challenges and opportunities. Prog. Mater. Sci. 117 https://doi.org/10.1016/ i.pmatsci.2020.100722.
- Consulting Collaborative, 2017. An overview of the N.A. aluminum extrusion market 2016 [WWW Document]. Consult. Collab. URL https://cdn.ymaws.com/www.aec.org/resource/resmgr/2017_SMW/1_Extrusion_Overview_-Brown.pdf (accessed 10.18.20).
- Cooper, D.R., 2013. Reuse of steel and aluminium without melting. University of Cambridge.
- Cooper, D.R., Rossie, K.E., Gutowski, T.G., 2017. The energy requirements and environmental impacts of sheet metal forming: an analysis of five forming processes. J. Mater. Process. Tech. 244, 116–135. https://doi.org/10.1016/j. imatprotec.2017.01.010.
- Cooper, D.R., Song, J., Gerard, R., 2018. Metal recovery during melting of extruded machining chips. J. Clean. Prod. 200, 282–292. https://doi.org/10.1016/j. jclepro.2018.07.246.

- Cullen, J.M., Allwood, J.M., 2013. Mapping the global flow of aluminum: from liquid aluminum to end-use goods. Environ. Sci. Technol. 47, 3057–3064. https://doi.org/ 10.1021/es304256s.
- Den Bakker, A.J., Katgerman, L., Van Der Zwaag, S., 2016. Analysis of the structure and resulting mechanical properties of aluminium extrusions containing a charge weld interface. J. Mater. Process. Technol. 229, 9–21. https://doi.org/10.1016/j. imatprotec.2015.09.013.
- Design News Staff, 2014. From the Ford GT to the F-150: Aluminum Extrusion Aids Auto Lightweighting [WWW Document]. Des. News. URL. https://www.designnews.com/materials-assembly/ford-gt-f-150-aluminum-extrusion-aids-auto-lightweighting (accessed 6.9.21).
- Dinsmore, E., 2018. Electric vehicles to transform aluminium demand [WWW Document]. URL https://www.crugroup.com/knowledge-and-insights/insights/201 8/electric-vehicles-to-transform-aluminium-demand /(accessed 6.9.21).
- European Aluminum Association, 2018. Environmental Profile Report [WWW Document]. URL https://european-aluminium.eu/resource-hub/environmental-profile-report-2018 (accessed 4.13.20).
- Ford Motor Company, 2013. Mechanical properties measurements after thermal processing of aluminum alloy.
- Ducker Worldwide, 2017. Aluminum Content in North American Light Vehicles 2016 To 2028 [WWW Document]. Ducker Worldw. URL. https://www.drivealuminum.org/research-resources/ducker2017 (accessed 6.9.21).
- Frischknecht, R., 2010. LCI modelling approaches applied on recycling of materials in view of environmental sustainability, risk perception and eco-efficiency. Int. J. Life Cycle Assess. 15, 666–671. https://doi.org/10.1007/s11367-010-0201-6.
- Furu, T., Østhus, R., Søreide, J., Myhr, O.R., 2017. A novel methodology for optimization of properties, costs and sustainability of aluminium extrusions. Mater. Sci. Forum 877, 625–632. https://doi.org/10.4028/www.scientific.net/MSF.877.625.
- Granta Design Limited, 2020. CES EduPack software.
- Gutowski, T.G., Sahni, S., Allwood, J.M., Ashby, M.F., Timothy, G.M., Ashby, F., Worrell, E., 2013. The energy required to produce materials: constraints on energy-intensity improvements, parameters of demand. Philos. Trans. Math. Phys. Eng. Sci. 371, 1–14. https://doi.org/10.1098/rsta.2012.0003.
- Haraldsson, J., Johansson, M.T., 2018. Review of measures for improved energy efficiency in production-related processes in the aluminium industry – from electrolysis to recycling. Renew. Sustain. Energy Rev. 93, 525–548. https://doi.org/ 10.1016/j.rser.2018.05.043.
- Hatzenbichler, T., Buchmayr, B., 2010. Finite element method simulation of internal defects in billet-to-billet extrusion. Proc. Inst. Mech. Eng. Part B J. Eng. Manuf. 224, 1029–1042. https://doi.org/10.1243/09544054JEM1830.
- ifu hamburg, 2020. Umberto LCA+.
- Ingarao, G., Priarone, P.C., Gagliardi, F., Di Lorenzo, R., Settineri, L., 2014.
 Environmental comparison between a hot extrusion process and conventional machining processes through a Life Cycle Assessment approach. Key Eng. Mater 622–623, 103–110. https://doi.org/10.4028/www.scientific.net/KEM.622-623.103.
- International Aluminum Institute, 2021. IAI current statistics [WWW Document]. URL https://www.world-aluminium.org/statistics/(accessed 9.6.21).
- ISO, 2016a. ISO Standard 14040 Environmental management Life cycle assessment — Principles and framework [WWW Document]. URL https://www.iso.org/ standard/37456.html (accessed 6.9.21).
- ISO, 2016b. ISO Standard 14044 Life cycle assessment Requirements and guidelines [WWW Document]. URL https://www.iso.org/standard/38498.html (accessed 6.9.21).
- Kaiser Aluminum, 2020. Kaiser Aluminum roundtable discussion.
- Kopec, G.M., Allwood, J.M., Cullen, J.M., Ralph, D., 2016. A general nonlinear least squares data reconciliation and estimation method for material flow analysis. J. Ind. Ecol. 20, 1038–1049. https://doi.org/10.1111/jiec.12344.
- Low, J.S.C., 2009. Cost modelling of the aluminum extrusion process. SIMtech Tech. Reports 10, 60–63.
- Macedonio, G., 2021. New, Danieli 40-MN Front-Loading Extrusion Press for PMS Aluminum [WWW Document]. Danieli. URL. https://www.danieli.com/en/news-media/news/new-danieli-40-mn-front-loading-extrusion-press-pms-aluminium_37_604. htm (accessed 6.9.21).
- Mag Specialties, 2019. Mag Specialties roundtable discussion.
- Masri, K., Warburton, A., 1998. Using optimization to improve the yield of an aluminium extrusion plant. J. Oper. Res. Soc. 49, 1111–1116. https://doi.org/10.1057/ palgrave.jors.2600616.
- Metson, J., 2011. Production of alumina, Fundamentals of Aluminium metallurgy: Production, Processing and Applications. Woodhead Publishing Limited, Sawston, UK, https://doi.org/10.1533/9780857090256.1.23.
- Mahmoodkhani, Y., Wells, M., Parson, N., Jowett, C., Poole, W., 2014. Modeling the formation of transverse weld during billet-on-billet extrusion 3470–3480. https:// doi.org/10.3390/ma7053470.
- MI Metals, 2019. MI Metals roundtable discussion.
- Misiolek, W.Z., Kelly, R.M., 2005. Extrusion of Aluminum Alloys (Ed.). In: Semiatin, S.L. (Ed.), ASM Handbook Metalworking: Bulk Forming. ASM International, pp. 522–527. https://doi.org/10.1361/asmhba0004015.
- Mulholland, E., 2016. Aluminum extrusion EPD background report.
- Nadel, S., Shepard, M., Greenberg, S., Katz, G., Almeida, A.T.De, 2002. Energy-Efficient Motor Systems: A Handbook On Technology, Program, and Policy Opportunities. Energy-Efficient Motor Systems: A Handbook On Technology, Program, and Policy Opportunities, 2nd ed. American Council for an Energy-Efficient Economy, Washington, D.C.
- Nieto, J.T., 2010. Feature Based Costing of Extruded Parts. University of Illinois at Urbana-Champaign.

- Norsk Hydro, 2020a. Aluminum extrusion alloys [WWW Document]. URL https://www.hydro.com/en-US/products-and-services/extruded-profiles/north-america-resources/extruded-aluminum-products/aluminum-extrusion-alloys /(accessed 5.31.21).
- Norsk Hydro, 2020b. Extruded aluminum rod [WWW Document]. URL https://www.hydro.com/en-US/products-and-services/extruded-profiles/north-america-resource s/extruded-aluminum-products/aluminum-rod/extruded-aluminum-rod /(accessed 6.9.21).
- In: Oberhausen, G.J., Christopher, A.A.A., Cooper, D.R., 2021. Reducing aluminum extrusion transverse weld process scrap (eds). In: Reducing aluminum extrusion transverse weld process scrap. Springer, Cham, https://doi.org/10.1007/978-3-030-75381-8 84.
- Page, I., 2020. Nemak Supplies New Battery Housings For the Mustang Mach-E [WWW Document]. Spotlight Met. URL. https://www.spotlightmetal.com/nemak-supplie s-new-battery-housings-for-the-mustang-mach-e-a-898095. /(accessed 6.9.21).
- Penny, T., Collins, T., Aumônier, S., Ramchurn, K., Thiele, T., 2013. Embodied energy as an indicator for environmental impacts – a case study for fire sprinkler systems. Sustainability in Energy and Buildings 555–565. https://doi.org/10.1007/978-3-642-36645-1 52.
- Rodriguez León, J.M., Stark, A., 2018. Current Trends in Aluminum Extrusion [WWW Document]. Spotlight Met. URL. https://www.spotlightmetal.com/current-trends-in-aluminum-extrusion-a-753015 (accessed 10.30.21).
- S&P Global Platts, 2019. Platts aluminum midwest premium explained [WWW Document]. URL https://www.spglobal.com/en/perspectives/platts-aluminum-midwest-premium-explained (accessed 6.9.21).
- Saha, P.K., 2000. Aluminum Extrusion Technology. ASM International, Materials Park, Ohio.
- Sattlethight, H., 2019. ARTICLE: North American Aluminum Extrusion Industry Hits Historic Record Shipment Highs [WWW Document]. Light Met. Age. URL. https://www.lightmetalage.com/news/industry-news/extrusion/north-american-alum inum-extrusion-industry-hits-historic-record-shipment-highs (accessed 6.9.21).
- Schlesinger, M.E., 2014. Aluminum Recycling, 2nd ed. CRC Press, Baca Raton, FL. 33487-2742.
- Schreiber, M., Sacristani, G., Gullotta, G., Fraternale, P., Breda, D., Balasmo-mi, C., 2016. Energy Saving in Extrusion Presses - Latest Developments. Eleventh International Aluminum Extrusion Technology Seminar & Exposition, Chicago, IL, pp. 471–488.
- Seow, Y., Rahimifard, S., Woolley, E., 2013. Simulation of energy consumption in the manufacture of a product. Int. J. Comput. Integr. Manuf. 26, 663–680. https://doi. org/10.1080/0951192X.2012.749533.
- Sheppard, T., 1999. Extrusion of aluminium alloys. Extrusion of Aluminium Alloys, 1st ed. Springer Science + Business Media, Dordrecht. https://doi.org/10.1007/978-1-4757-3001-2
- Sherman, E., 2009. New Apple Technology to Produce Seamless Metal iPhone Case [WWW Document]. CBS News. URL. https://www.cbsnews.com/news/new-apple-te-chnology-to-produce-seamless-metal-iphone-case (accessed 6.9.21).

- SMS Group, 2020. ecoDraulic: energy efficient operation of an extrusion press for aluminum [WWW Document]. URL https://www.sms-group.com/sms-group-maga zine/overview/ecodraulic-energy-efficient-operation-of-an-extrusion-press-for-alum inum /(accessed 6.11.21).
- Superior Aluminum, 2019. Superior Aluminum roundtable discussion.
- Sutherland, J., Skerlos, S., Haapala, K., Cooper, D., Zhao, F., Huang, A., 2020. Industrial sustainability: reviewing the past and envisioning the future. J. Manuf. Sci. Eng. 142, 1–33. https://doi.org/10.1115/1.4047620.
- Tekkaya, A.E., Schikorra, M., Becker, D., Biermann, D., Hammer, N., Pantke, K., 2009. Hot profile extrusion of AA-6060 aluminum chips. J. Mater. Process. Technol. 209, 3343–3350. https://doi.org/10.1016/j.jmatprotec.2008.07.047.
- Thumb Tool & Engineering, 2018. Thumb tool & engineering roundtable discussion.

 Tomczyk, A., 2019. Creating cost-effective extruded aluminum component solutions webinar
- U.S. Bureau of Labor Statistics, 2021a. Electricity per KWH in Midwest urban, average price, not seasonally adjusted.
- U.S. Bureau of Labor Statistics, 2021b. Utility (piped) gas per therm in Midwest urban, average price, not seasonally adjusted.
- U.S. Bureau of Labor Statistics, 2020a. 51-4021 Extruding and drawing machine setters. Operators, and Tenders. Metal and Plastic.
- U.S. Bureau of Labor Statistics, 2020b. "Employer costs for employee compensation -December 2020".
- U.S. Department of Energy, 2003. Alcoa : plant-wide energy assessment finds potential savings at aluminum extrusion facility.
- UN, 2018. UN comtrade database 2018.
- US Environmental Protection Agency, 2020. Inventory of U.S. greenhouse gas emissions and sinks.
- Wernet, G., Bauer, C., Steubing, B., Reinhard, J., Moreno-Ruiz, E., and Weidema, B., 2016. EcoInvent Version 3.
- Wünning, J.G., 2007. Energy-saving possibilities for gas-fired industrial furnaces. Heat Treat. Prog. 7, 37–42.
- Zhang, C., Dong, Y., Wang, C., Zhao, G., Chen, L., Sun, W., 2017. Evolution of transverse weld during porthole extrusion of AA7N01 hollow profile. J. Mater. Process. Technol. 248, 103–114. https://doi.org/10.1016/j.jmatprotec.2017.05.017.
- Zhu, Y., Chappuis, L.B., De Kleine, R., Kim, H.C., Wallington, T.J., Luckey, G., Cooper, D. R., 2021. The coming wave of aluminum sheet scrap from vehicle recycling in the United States. Resour. Conserv. Recycl. 164, 105208 https://doi.org/10.1016/j.resconrec.2020.105208.
- Zhu, Y., Syndergaard, K., Cooper, D.R., 2019. Mapping the annual flow of steel in the United States. Environ. Sci. Technol. 53, 11260–11268. https://doi.org/10.1021/acs.est 0b01016
- Zyp Coatings, 2021. Boron nitride spray [WWW Document]. URL https://www.zypcoatings.com/product/bn-glass-release-spray (accessed 6.9.21).